STAR Protocols

Protocol

Protocol for fabricating and characterizing microvessel-on-a-chip for human umbilical vein endothelial cells

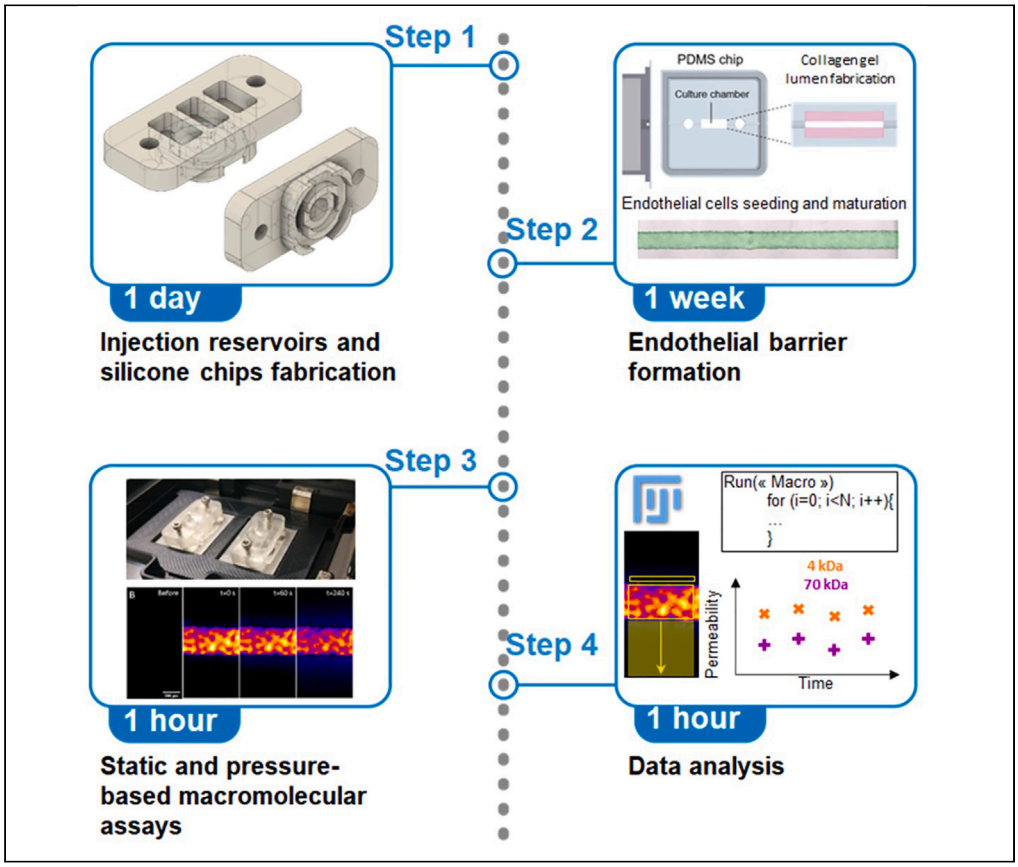

Organ-on-a-chip technologies enable the fabrication of endothelial tissues, so-called microvessels (MVs), which emulate the endothelial barrier function in healthy or disease conditions. In this protocol, we describe the fabrication of perfusable open-chamber style MVs embedded in collagen gels. We then report a simple technology to characterize the MV barrier properties in static or under pressure based on fluorescence confocal imaging. Finally, we provide quantification techniques that enable us to infer the structure of MV paracellular pores.

Publisher's note: Undertaking any experimental protocol requires adherence to local institutional guidelines for laboratory safety and ethics.

Jean Cacheux, Tadaaki Nakajima, Daniel Alcaide, Takanori Sano, Kotaro Doi, Aurélien Bancaud, Yukiko T. Matsunaga

abancaud@laas.fr (A.B.)
mat@iis.u-tokyo.ac.jp (Y.T.M.)

Highlights

Instructions for fabricating microvessel-on-achip of 200 μm in diameter

Tools to assess barrier function by monitoring fluorescence redistribution

Steps to extract the structure of the barrier from fluorescence microscopy data

Characterization of the barrier quality based on its response to intraluminal pressure

Cacheux et al., STAR Protocols 5, 102950
June 21, 2024
https://doi.org/10.1016/j.xpro.2024.102950

STAR Protocols

CellPress

Protocol

Protocol for fabricating and characterizing microvessel-on-a-chip for human umbilical vein endothelial cells

Jean Cacheux,[1,2,4] Tadaaki Nakajima,[1] Daniel Alcaide,[1,2] Takanori Sano,[1] Kotaro Doi,[1] Aurélien Bancaud,[1,2,3,5,*] and Yukiko T. Matsunaga[1,2,*]

[1]Institute of Industrial Science, The University of Tokyo, Tokyo 153-8505, Japan

[2]LIMMS, CNRS-IIS UMI 2820, The University of Tokyo, Tokyo 153-8505, Japan

[3]CNRS, LAAS, 7 Avenue du colonel Roche, 31400 Toulouse, France

[4]Technical contact

[5]Lead contact

*Correspondence: abancaud@laas.fr (A.B.), mat@iis.u-tokyo.ac.jp (Y.T.M.)
https://doi.org/10.1016/j.xpro.2024.102950

SUMMARY

Organ-on-a-chip technologies enable the fabrication of endothelial tissues, so-called microvessels (MVs), which emulate the endothelial barrier function in healthy or disease conditions. In this protocol, we describe the fabrication of perfusable open-chamber style MVs embedded in collagen gels. We then report a simple technology to characterize the MV barrier properties in static or under pressure based on fluorescence confocal imaging. Finally, we provide quantification techniques that enable us to infer the structure of MV paracellular pores.

For complete details on the use and execution of this protocol, please refer to Cacheux et al.[1]

BEFORE YOU BEGIN

The protocol below describes the specific steps for fabricating and characterizing microvessel (MV) with human umbilical vein endothelial cells (HUVECs), as initially developed by Pauty et al.[2,3] It can be adapted to other type of endothelial cells such as human brain endothelial cells; human lymphatic endothelial cells,[4] and epithelial cells (Caco-2[5]; MDCK). The protocol starts with a complete strategy to fabricate MVs, then describes the strategy to perform the macromolecular permeability assay in static or pressure conditions, and finally presents the method to analyze the resulting datasets.

As a starting point, we provide an overview of the principles underlying the connection between MV barrier structure (i.e., the geometry of paracellular pores) and the molecular transport across the vascular wall. In the conventional permeability assay, the characterization of endothelial barrier function relies on the measurement of the flux of tracers crossing the tissue. This flux is inferred by counting the number of fluorescent tracers that diffuse out from the MV lumen per unit of time. This flux is then divided by the apical to basal concentration difference in order to define the diffusive permeability $\mathcal{L}_D$. Normalized with the diffusion coefficient of the probe D_{probe}, it can be shown that $\mathcal{L}_D$ depends on the structure of paracellular pores:

$$\frac{\mathcal{L}_D}{D_{probe}} = n\pi\frac{{r_p}^2}{\delta_D} \qquad \text{(Equation 1)}$$

where n is the density of pores, r_p the radius of pores, and δ_D is the barrier thickness. We provide methods to infer these structural parameters following the approach of our report,[1] and indicators of the quality of the endothelial barrier.

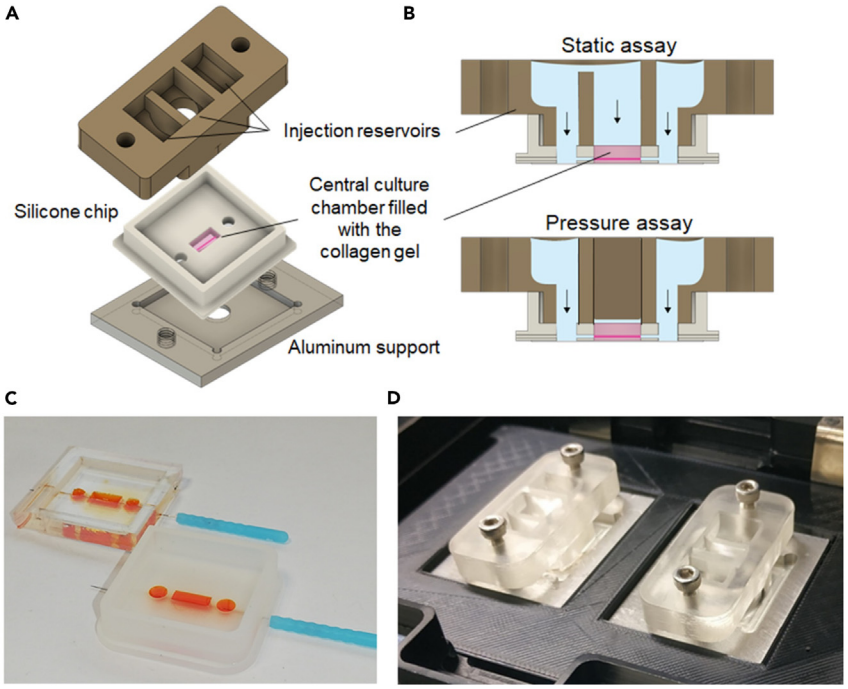

Figure 1. Setup for the static and pressure macromolecular permeability assays

(A) Scheme of the 3D printed injection reservoir and its integration on the MV chip with the aluminum support plate.

(B) Cross-sectional view of the devices for the static and hydrostatic pressure assay. The difference in fluid height in the pressure assay is 1 cm, equivalently the intraluminal pressure is 100 Pa.

(C) Photographs of the MV chips as described in this report or as in the work of Pauty et al.[2,3] Each well is stained with red dye at the condition of needle insertion.

(D) Photographs of the actual setup for the devices placed on a microscope stage.

Fabrication of the injection reservoirs by 3D printing

Timing: 0.5 day

In this section, the design and fabrication of 3D injection reservoirs is described.

Alternatives: Whenever utilizing MV chips with different specifications, a new design should be implemented with a 3D CAD software such as Fusion 360 (Autodesk Inc., San Francisco, USA) or equivalent. Also, the devices for the static or pressure assays (Figure 1) can be fabricated by 3D-printing (as described below) or by conventional machining.

1. Slicing of the reservoirs design.
   a. Upload the STL file (Data S1 and Figure S1) of the reservoirs design to Chitubox software.
   b. Slice the design with the following parameters, which have been determined for our water-soluble resin (see the key resources table).
   c. Export your file to CTB format.

   Alternatives: File format and printing parameters should be adapted according to the 3D printer and associated resist.

2. 3D-printing.
   a. Calibrate the 3D printer.
   b. Fulfill the tank with resin.

Parameter	Value
Bottom exposure (s)	8
Normal exposure (s)	2
Layer height (μm)	50
Z lifting distance (mm)	15
Z lifting speed (mm/min)	100
Z retract speed (mm/min)	200
Rest time after retract (s)	0

c. Upload you CTB file to the 3D printer.
d. Start printing.

3. Post-processing.
   a. Clean the 3D-printed reservoirs with 70% ethanol and milliQ water.
   b. Expose for 5 h to UV light (405 nm, 600 W).
   c. Bake at 70°C overnight.
   d. Store in 100 mL PBS 1×.

Note: These post-processing steps ensure the biocompatibility of the 3D-printed reservoirs.

⚠ CRITICAL: Use a UV light source with a wavelength adequate to complete the reticulation of the resist.

Alternatives: Any other 3D-printer and resist could be used, adjust the post-processing step according to your material.

Fabrication of the silicone chips

Timing: 0.5 day

In this section, we provide the details for the fabrication of silicone chips with a guide for acupuncture needles.

4. Cut the 250 μm-thick silicone sheet with the following parameters (laser speed = 150 mm/s, P_{min} = 30 W and P_{max} = 36.5 W) according to the design of the first layer (Figures 1B and S2).
5. Cut the 1.6 mm-thick silicone sheet with the following parameters (laser speed = 25 mm/min, P_{min} = 34 W and P_{max} = 37 W) according to the design of the second and third layers (Figure S2).
6. Engrave the second layer of 1.6 mm-thick silicone sheets with the following parameters (laser speed = 220 mm/min, P_{min} = 20 W and P_{max} = 38 W).
7. Clean the silicone sheets with water and soap.
8. Perform air plasma for 3 min for silicone surface activation on the first two layers.
9. Repeat step 5 for the previously bonded layers and the third layer.
10. Incubate the resulting system for 2 h at 120°C.
11. Cut individual chips with a cutter.
12. Perform air plasma for 3 min to bond the silicon chips to a 20 × 20 mm^2 glass slide.
13. Incubate the resulting system for 2 h at 120°C.

HUVECs culture

Timing: 3 days

Note: The following steps are performed in sterile conditions using a biosafety culture hood

In this section, we report the details to prepare the endothelial cell culture before its loading into the MV chip.

14. Upon purchase, seed HUVECs in a 100-mm tissue culture polystyrene dishes (TCPS; passage 1, P1). Culture HUVECs to confluency, split by 4-fold at each passage, and freeze the sample in liquid nitrogen using vials of 10^6 HUVECs in 1 mL in liquid nitrogen. Use HUVECs from P4 to P7, but P4 and P5 is recommended.
15. Thaw a frozen vial by placing it into a 37°C water bath.
16. Transfer the entire sample in a 15 mL centrifuge tube containing 5 mL of media. Perform the transfer dropwise at a rate of 1 drop/second.

⚠ CRITICAL: Cells from frozen stocks must be transferred into fresh medium just till the last ice crystal remains.

17. Mix the cells in the tube and centrifuge at 500 g for 3 min.
18. Remove the supernatant, resuspend in 6 mL of fresh medium, and thoroughly break the pellet by gently tapping the base of the tube with the tips and mix by pipetting up and down.
19. Prepare six 60 mm TCPS with 4 mL of medium.
20. Add 1 mL of the cell preparation into each TCPS.

⚠ CRITICAL: Use dropwise addition of the cell preparation to obtain a uniform seeding in the TCPS.

21. Incubate the cells on TCPS at 37°C and 5% CO_2 for 3 h.
22. Gently remove and replace the 5 mL of medium.
23. Culture the cells until reaching 90% confluency by changing media every other day.

KEY RESOURCES TABLE

REAGENT or RESOURCE	SOURCE	IDENTIFIER
Chemicals, peptides, and recombinant proteins		
PBS 10× solution	Fujifilm Wako	048-29805
Glutaraldehyde	Sigma-Aldrich	G6257
Paraformaldehyde, 4% in PBS	Thermo Fisher Scientific	J61899.AK
Hank's balanced salt solution 10×	Sigma-Aldrich	H1641-500ML
Bovine serum albumin (BSA)	Sigma-Aldrich	9048-46-8
Cellmatrix type I-A or I-P collagen	Nitta Gelatin	631-00651/631-00661
Sodium hydroxide	Sigma-Aldrich	1310-73-2
Sodium hydrogen carbonate	Sigma-Aldrich	144-55-8
HEPES	Sigma-Aldrich	7365-45-9
Trypsin-EDTA	Fujifilm Wako Pure Chemical	208-17251
Fibronectin	Biomedical Technologies, Inc.	BT-226S
Dextran 500 kDa	Sigma-Aldrich	31392-10G
Dextran 4 kDa fluorescein	Sigma-Aldrich	68059
Dextran 70 kDa rhodamine	Sigma-Aldrich	46945
3-Aminopropyltriethoxysilane	Sigma-Aldrich	440140-100ML
VE-Cadherin monoclonal antibody (rabbit)	Cell Signaling Technology	D87F2
Alexa Fluor 568 goat anti-rabbit	Thermo Fisher Scientific	A-11011
Alexa Fluor 488 phalloidin	Thermo Fisher Scientific	A12379
Hoechst 33342	Thermo Fisher Scientific	H3570

(*Continued on next page*)

Continued		
REAGENT or RESOURCE	SOURCE	IDENTIFIER
Experimental models: Cell lines		
HUVECs	Lonza, Basel, Switzerland	C2519A
EGM-2 medium	Lonza, Basel, Switzerland	CC-3162/6
Software and algorithms		
Fiji	ImageJ	1.53t
Macro Fiji	Authors	https://doi.org/10.17632/2rs7y84njn.1
FeatureJ plugin for ImageJ	https://imagescience.org/meijering/software/featurej/	N/A
Other		
Acupuncture needle 200 μm	Seirin, Shizuoka, Japan	No.8, J-type
Strainer	Falcon, Corning, NY, USA	352235
0.2 μm Minisart syringe filter	Sartorius	17597-K
3D stereolithography photoresist	Expert Material Series	N/A
Aluminum support	House made	Supplementary Material
Silicone sheet (thickness: 250 μm)	MVQ Silicones GMBH	SIP0,25HT6240GK
Silicone sheet (thickness: 2 mm)	MVQ Silicones GMBH	SIP1,6HT6240GK
3D stereolithography printer	Elegoo	Mars 3
Basic plasma cleaner	Harrick Plasma	PDC-32G (115V)
Laser cutting system	LaserSystem	PURELASER 7050
Dessicator	Sigma-Aldrich	BAF424002241
Confocal microscope with a 10× and a 40× water immersion objective (numerical aperture = 0.4 and 1.2, respectively).	Carl Zeiss	LSM 700

MATERIALS AND EQUIPMENT

Collagen reconstitution buffer		
Reagent	Final concentration	Amount
Sodium hydroxide	50 mM	20.0 mg
Sodium hydrogen carbonate	260 mM	218.4 mg
HEPES	200 mM	476.6 mg
Total (in milliQ water)	**10×**	**10 mL**
Aliquots in ten 1 mL vials, store at 4°C and use within 4 months.		

Sterilized PBS 1×

- Dilute PBS 10× with milliQ water and autoclave.

1% BSA solution

- Add 0.1 g of BSA in 10 mL of PBS 1×.
- Sterilize with 0.2 μm filters.

Store at 4°C and use within one month.

Antibody solutions

- Add 1 μL of primary antibody in 200 μL of 1% BSA solution for the primary antibody solution.
- Add 1 μL of secondary antibody in 500 μL of 1% BSA solution for the secondary antibody solution.

10–50 μg/mL fibronectin solution

- Dilute fibronectin stock solution (1 mg/mL) by one hundred-fold with PBS 1×.

Store at 4°C.

3% dextran EGM-2 solution

- Weight 300 mg of dextran 500 kDa.
- Add 10 mL of warm EGM-2 medium.
- Vortex until dextran is dissolved.
- Sterilize with 0.2 μm filters.

Fluorescent 4 kDa and 70 kDa dextran solution

- Weight 10 mg of 4 kDa FITC-conjugated dextran and 70 kDa rhodamine-B-conjugated dextran.
- Add 1 mL of PBS 1×.
- Mix well.

STEP-BY-STEP METHOD DETAILS

Silicone chip and needle preparation

Timing: 1 h

The following steps describe the surface modification of silicone chips in order to covalently graft the collagen gel in the MV chip. This protocol ensures that the chips are not leaky during the permeability assays.

Note: 4 to 6 silicone chips and needles can be prepared at the same time.

1. Treat the silicone chips and acupuncture needles with air plasma for 3 min.

Note: Next step is performed under a chemical hood.

2. Place the chips in a vacuum chamber with 40 μL of 3-aminopropyltriethoxysilane for 30 min at room temperature.
3. Bake the chips at 70°C for 30 min.

Note: Next steps are performed under a culture hood.

4. Incubate the acupuncture needles with the 1% BSA solution for 15 min.
5. Dispense 40 μL of the 2.5% glutaraldehyde (GA) solution into both the central culture chamber and the lateral reservoirs of the silicone chip, and wait for 5 s.
6. Rinse the GA solution by adding 1 mL of milliQ water 5 times.
7. Dry silicone chips and needles with air.

Note: Glutaraldehyde is highly toxic and should be manipulated carefully and discarded properly.

⚠ CRITICAL: Exposure time of the silicone chips to GA should be minimal to avoid future cell intoxication.

Collagen gel channel fabrication

Timing: 1 h

The next steps describe the fabrication of the collagen gel lumen.

⚠ CRITICAL: Neutralized collagen solution must be stored in an ice bucket to slow down the gelation process. Solutions are prepared and used within 15 min.

8. Prepare 0.5 mL of collagen solution by mixing 50 μL of Hank's solution, 400 μL of Cellmatrix Type I-A/I-P Collagen and 50 μL of collagen reconstitution buffer in volume fraction.
9. Mix thoroughly by pipetting.
10. Centrifuge the solution for 15 s to eliminate bubbles, then place the sample back on ice.

Note: We use 0.5 mL of collagen solution to prepare 6 MV chips.

11. Add 5 μL of collagen solution in each lateral reservoir and 30 μL in the central culture chamber.
12. Insert the acupuncture needle through guiding channel in the silicone chip.
13. Incubate the silicone chips at 37°C and > 95% humidity for 30–45 min.
14. Fill the entire silicone chip volume by adding 1 mL of PBS 1×.
15. Gently remove the needle.
16. Store the collagen gel scaffolds in the cell culture incubator for one night at least, see troubleshooting 1.

Microvessel fabrication

Timing: 2 h

This section describes the loading of HUVECs in the MV chip.

17. Wash out the 1 mL PBS 1× by aspiration with a pipette or with vacuum.
18. Add 1 mL of fresh PBS 1×.
19. Remove the collagen solution in the lateral reservoirs.
20. Rinse the chip with fresh PBS 1× two times in order to remove collagen gel debris.

CAUTION: Gel removal should be done with PBS in the chip to avoid the formation of air bubbles in the collagen tube.

21. Add 10 μL of 1% fibronectin in each reservoir and on the top of the collagen gel, and incubate for 30 min at 37°C.
22. In the meantime, take out the HUVEC-cultured in TCPS from the incubator.
    a. Aspirate the medium and rinse twice with 5 mL of PBS 1×.
    b. Add 500 μL of trypsin-EDTA, shake gently and incubate 5 min at 37°C.
    c. Collect the cells in 2 mL (2 × 1 mL) of EGM-2 medium in a 15 mL tube
    d. Pipet up and down to disrupt aggregates.
    e. Use 10 μL of the cell suspension for counting.
    f. Centrifuge for 3 min at 500 g.
    g. Remove the EGM-2 medium and resuspend the cell pellet in the appropriate volume of the 3% dextran EGM-2 medium to obtain 10^7 cells/mL.

Note: *e.g.*, if after counting, the collected cells concentration is 5×10^5 cells/mL, the pellet after centrifugation contains 1.5 million cells. To reach 10^7 cells/mL, the cells pellet must be

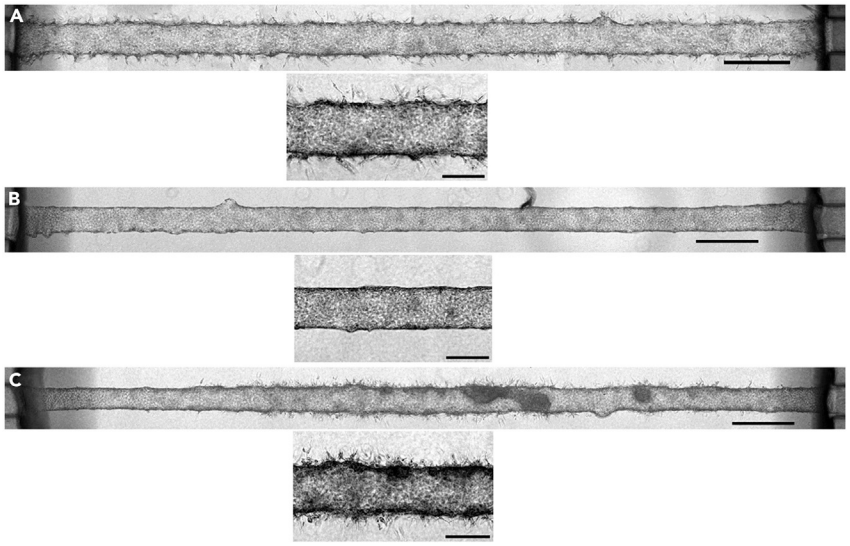

Figure 2. Bright field micrographs of the MV after 2 days of culture

(A) The 6 mm-long MV can be characterized by a clear and sharp intensity profile under the microscope. The bottom panel is a zoom-in.

(B) Same as (A) with a low-quality barrier because the number of HUVECs loaded in the lumen is insufficient (see corresponding characterization in the upper panel of Figure 3).

(C) Same as (A) with an overloading of HUVECs. Scale bars represent 500 μm for the entire MVs and 200 μm for the zoom-ins.

resuspended in 150 μL of 3% dextran EGM-2. The concentration of cells is adapted when dealing with other cell types. For instance, we use 4×10^6 cells/mL with Caco-2.

23. Take out the silicone chips from the incubator.
24. Gently aspirate the fibronectin from the lateral reservoirs.
25. Wash with 50 μL of the 3% dextran EGM-2 solution.
26. Discard the 3% dextran EGM-2 solution, leaving a minimal fluid volume of 1 μL in each lateral reservoir.
27. Pass the cell suspension through the cell strainer to singularize the cells.
28. Inject 10 μL of the HUVECs solution in one of the lateral reservoirs and wait for the flow to equilibrate.
29. Leave the chip in the culture hood for 10 min in order to allow a continuous permeation flow through the collagen forced the evaporation of water. Observe the vessel under the microscope to check the cell density, see troubleshooting 2 and examples in Figure 2.

Note: The evaporation of the liquid through the collagen favors the aspiration of a large number of cells in the lumen and the obtention of endothelial tissues with high cell density.

30. Invert the chips upside down, and incubate for 5 min at 37°C.

Note: The inversion is critical to insure the homogeneous coverage of the cells on the upper and lower halves of the vessel.

31. Pipet out the liquid from the reservoir opposite to that of the loading step, leaving 1 μL in each lateral reservoir.
32. Repeat steps 29 to 32, and make sure that the liquid is flowing through the lumen, see troubleshooting 3.

33. Add 1 mL of fresh EGM-2 medium on top of the silicone chip.
34. Incubate for 3 h and change the medium.
35. Fill the two lateral needle guides with an acupuncture needle of 300 μm in diameter.
36. Culture the MV and change medium every other day.

Note: Most of our experiments are carried out after 2–4 days after fabrication. Barrier function can be assessed after 7 days. Yet, we notice a variability after 5–7 days of culture with some MV that hold up quite well, but others starting to present discontinuities in their barrier due to cell death.

Permeation assay in static and pressure conditions

Timing: 30 min

Note: The protocols for the static and pressure assays are nearly identical. The only distinction between these two experiments arises from the modification of the 3D printed injection reservoirs. In the static assay, a uniform hydrostatic pressure is applied from both sides of the endothelial cell barrier (upper panel of Figure 1B). Conversely, the pressure assay introduces a pressure gradient, as the reservoir onto the collagen is left empty (lower panel of Figure 1B).

This section describes the operation of the permeation assay with a confocal microscope.

37. Place the MV chip on an aluminum support and screw the 3D-printed injection reservoir device on top of it (Figure 1D).
38. Add 500 μL of EGM-2 media in the 3D-printed device and wait for the flow to equilibrate.

CAUTION: Pipette up and down slowly the medium in the inlets to remove any potentially stacked bubble.

39. Place the system on the confocal microscope.

CAUTION: The quantification of the macromolecular assay can be performed with a bright field microscope. However, it does not permit the extraction of accurate quantitative permeability measurements, as the fluorescence signal within the lumen is distorted by out-of-focus fluorescence generated by dyes escaping into the collagen gel.

40. Set the optical section to 10–20 μm (i.e., 5–10% of the vessel diameter) and the inter-frame time interval to 10 s with an image size of 512 × 512 pixels (e.g., 1.28 × 1.28 mm^2). It can be useful to perform multiple position acquisition to assess the permeation properties more globally.

Note: The time interval should be selected according to the quality of the barrier. If the number of molecules that escape from the lumen is low, the signal increases slowly in the collagen gel and it is recommended to increase the inter-frame interval to 30 s.

41. Load 30 μL of fluorescent dextran solution in one inlet of the lumen through the reservoir.
42. Run the acquisition for 3–4 min, focusing the objective at the equatorial plane of the lumen.
43. Remove the 3D-printed device after 3–4 min of image acquisition, rinse the chip with fresh medium, and place the sample in the incubator for 30 min, see troubleshooting 4.
44. Repeat steps 39 to 44 with the 3D-printed device for the pressure assay.

Immunostaining of microvessels

Timing: 2 days

This section describes the protocol to perform immune-confocal microscopy on MVs.

45. Remove the medium in the chip and replace it with the 4% paraformaldehyde (PFA) solution for 30 min.
46. Rinse the PFA solution with PBS six times consecutively.
47. Incubate with the 1% BSA solution for 4 h at least at room temperature.
48. Incubate with the VE-Cad primary antibody (Rabbit) for 4 h at least at room temperature.
49. Rinse with PBS six times consecutively.
50. Incubate with the secondary antibody (Goat anti-Rabbit) for 4 h at least at room temperature.
51. Rinse with PBS six times consecutively.
52. Incubate with Hoechst (1:1000) and Alexa 488 phalloidin (1:1000) diluted in PBS for 1 h.
53. Rinse with PBS two times consecutively.
54. Perform confocal microscopy with a z-stack size set to 1 μm the confocal thickness.

Data analysis

Timing: 30 min

This section provides the method to extract the diffusive permeability of MVs and infer the structure of paracellular pores.

55. Import image sequence data in ImageJ, correct the orientation of the vessel to horizontal if needed.
56. Create separate image sequences for each fluorophore in static conditions.
57. Run the macro to extract the vessel radius r_{0D}, and the diffusive permeability $\mathcal{L}_D$ for both sides of the vessel at each time step of the video.

Note: The macro automatically defines the edges of the vessel, then measures the intraluminal dye concentration, the concentration in the basal layer, and the integral of the fluorescence signal around the MV.

58. Compute the average diffusive permeability for the two fluorophores in static conditions $\mathcal{L}_{D4\ kDa}$ and $\mathcal{L}_{D70\ kDa}$.

Note: These parameters are in the range of 50 $\pm$ 30 and 7 $\pm$ 4 nm/s, respectively. A poor barrier, as shown in the upper panel of Figure 3, is characterized by a diffusive permeability of 500 nm/s for the 4 kDa dextran.

59. Normalize these quantities to the diffusion coefficient of the corresponding probe, e.g., $\mathcal{L}_{D4\ kDa}/D_{4kDa}$. Note the values of 244 +/- 25 and 62 +/- 6 $\mu m^2/s$ for D_{4kDa} and D_{70kDa} in collagen gels, respectively (see the calibration in ref. 1).
60. Compute the ratio of $(\mathcal{L}_{D70\ kDa}/D_{70kDa})/(\mathcal{L}_{D4\ kDa}/D_{4kDa})$ to determine the relative hindrance coefficient (see Equation 4 below).

Note: This ratio is spanning 0.2 to 1 from high- to poor-quality barriers, respectively.

61. Determine the pore size r_p by numerical inversion of the relative hindrance, as described in ref. 1.

Note: r_p is on the order of 20 nm for a high-quality barrier.

62. Measure the barrier thickness based on the VE-Cadherin immunofluorescence confocal micrograph (Figures 4A and 4B).

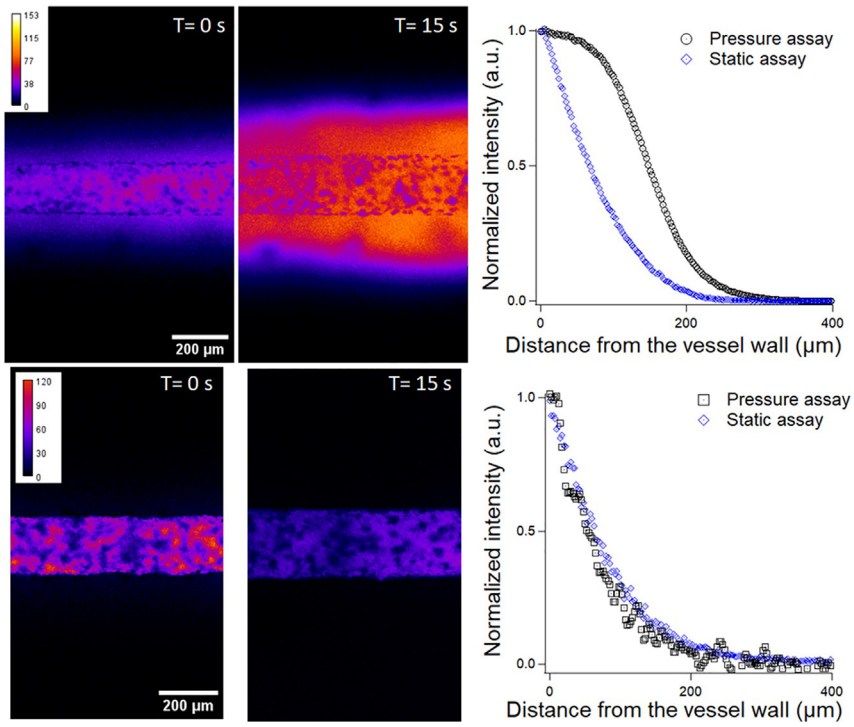

Figure 3. Representative FITC-dextran (4 kDa) concentration profiles after 15 s in a leaky and semi-permeable barrier (upper and lower panel, respectively)

In each panel, the left and right confocal micrographs represent the readout of the static and pressure assays, respectively. The respective normalized intensity profiles *vs.* position in the collagen gel are extracted for both assays, as indicated in the caption. Note that this data corresponds to Figures 2A and 2B for the semi-permeably and leaky MV, respectively.

Note: The barrier thickness δ_D is typically 3 µm (Figure 4C), as confirmed by transverse electron microscopy. The pore density can then be inferred using Equation 1. Its value is in the order of unity per μm^2.

63. Run the macro for the permeability assay in pressure conditions and extract the vessel radius r_{0P} and the diffusive permeability $\mathcal{L}_P$ (Equation 6, below).

Note: The change in MV diameter associated to an intraluminal pressure of 100 Pa is 25% (see the lower panel of Figure 3 for an example).

64. Confirm the quality of the barrier by computing $\mathcal{L}_P/\mathcal{L}_D$.

Note: This quantity should not be much greater than r_{0P}/r_{0D} for high quality barriers.

EXPECTED OUTCOMES

Before conducting experiments, it is crucial to verify that the injection reservoirs are properly connected to the silicone chip and the MV barrier, as illustrated in Figure 1. Note that leaks are immediately observed as the liquid is spilled outside of the silicon chip.

Quality control of MV fabrication can be qualitatively inferred from bright field micrographs because good barriers are characterized by a clear and sharp intensity profile (upper panel of Figure 2). The contrast readily diminishes if the injection load is insufficient (middle panel of Figure 2).

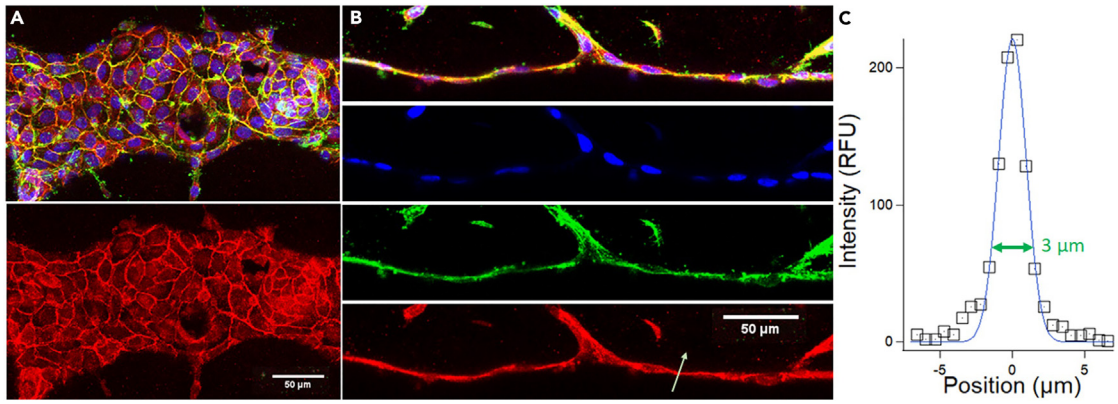

Figure 4. Immunoconfocal micrograph of microvessels

(A) Maximum intensity projection of confocal micrographs obtained by staining MV with phalloidin for the detection of fibril actin in green, nuclear DNA in blue, and VE-Cadherin in red. The MV were fixed just after the static and pressure assays. The projection represents the bottom of the lumen.

(B) The same vessel is observed on its side. The scale bars correspond to 50 µm.

(C) The square markers and solid line represent the intensity that were sampled from the contour shown with an arrow in panel (B) and fitted to a Gaussian function.

The barrier quality can be quantitatively assayed by analyzing the images of the macromolecular assays. Indeed, if transport is primarily governed by diffusion in the static and pressure assays, both profiles should exhibit the same spatial distribution after normalization. Figure 3 shows the comparison of a leaky MV *vs.* a quality barrier and their associated readouts with the static and pressure assays (upper and lower panels, respectively).

QUANTIFICATION AND STATISTICAL ANALYSIS

Using the outputs of macromolecular assays in static conditions, the diffusive permeability is obtained with the following expression:

$$\mathcal{L}_D = J_D/(2\pi r_{0D}(C_{in} - C_{out})) \quad \text{(Equation 2)}$$

with r_{0D} the vessel radius. As explained in the introduction of this manuscript, the diffusive permeability is related to the structure of paracellular pores (Equation 1). Taking into account the excess of friction due to the confinement in the narrow pores, Equation 2 can be expressed as:

$$\mathcal{L}_D = n\pi \frac{r_p^2}{\delta_D} D_{probe} \mathcal{H}(r_{probe}/r_p) \quad \text{(Equation 3)}$$

with $\mathcal{H}(r_{probe}/r_p)$ the hindrance parameters, which is a function of r_{probe}/r_p with r_{probe} the hydrodynamic radius of the dye. By computing the ratio of the diffusive permeabilities measured with the two probes and knowing r_{probe}, we can determine the radius of the pores r_p using an inverse method. Assuming the pores have the same geometry and density no matter the size the probe, we use the expression of the hindrance factor in ref. 6, and compute the hindrance of both probes:

$$\frac{(\mathcal{L}_{D70\ kDa}/D_{70kDa})\left(\frac{r_{70kDa}}{r_p}\right)}{(\mathcal{L}_{D4\ kDa}/D_{4kDa})\left(\frac{r_{4kDa}}{r_p}\right)} =$$

$$\left\{1 + \frac{9}{8}\frac{r_{70kDa}}{r_p} ln\left(\frac{r_{70kDa}}{r_p}\right) - 1.56034\frac{r_{70kDa}}{r_p} + 0.528155\left(\frac{r_{70kDa}}{r_p}\right)^2 + 1.91521\left(\frac{r_{70kDa}}{r_p}\right)^3 - 2.81903\left(\frac{r_{70kDa}}{r_p}\right)^4\right.$$

$$\left. + 0.270788\left(\frac{r_{70kDa}}{r_p}\right)^5 + 1.0115\left(\frac{r_{70kDa}}{r_p}\right)^6 - 0.435933\left(\frac{r_{70kDa}}{r_p}\right)^7\right\} \Big/$$

$$\left\{1+\frac{9}{8}\frac{r_{4kDa}}{r_p}ln\left(\frac{r_{4kDa}}{r_p}\right)-1.56034\frac{r_{4kDa}}{r_p}+0.528155\left(\frac{r_{4kDa}}{r_p}\right)^2+1.91521\left(\frac{r_{4kDa}}{r_p}\right)^3-2.81903\left(\frac{r_{4kDa}}{r_p}\right)^4\right.$$

$$\left.+0.270788\left(\frac{r_{4kDa}}{r_p}\right)^5+1.0115\left(\frac{r_{4kDa}}{r_p}\right)^6-0.435933\left(\frac{r_{4kDa}}{r_p}\right)^7\right\} \quad \text{(Equation 4)}$$

Note that the radius of the 4 kDa and 70 kDa dextran probes is 1.5 and 6.2 nm, respectively. Upon application of intraluminal pressure, the flux $J_P(t)$ results from the cumulative effect of convection and diffusion in the pores. Defining v_0 the velocity of the flow in paracellular space, we can use the Patlak expression of the flux[7]:

$$J_P(t) = 2\pi r_{0P} C_{in} v_0 \left(1+\frac{1-C_{out}/C_{in}}{e^{v_0/\mathcal{L}_P}-1}\right) \quad \text{(Equation 5)}$$

Note that we use a different diffusive permeability coefficient $\mathcal{L}_P$ due to the possible change in pore geometry. For endothelial tissues, and even more so for epithelia, the contribution of diffusion is dominant over that of convection. Hence, Equation 4 can be written as:

$$J_P(t) \approx 2\pi r_{0P} \mathcal{L}_P (C_{in} - C_{out}) \quad \text{(Equation 6)}$$

The change in diffusive permeability under pressure is mainly due to the change in barrier thickness δ_P but not by the change in pore radius, according to the deformable monopore model:

$$\mathcal{L}_P = n\pi \frac{r_p^2}{\delta_P} D_{probe} \mathcal{H}(r_{probe}/r_p) = \mathcal{L}_D \frac{\delta_P}{\delta_D} \quad \text{(Equation 7)}$$

The difference of barrier thickness in the static and pressure assays adds another parameter in the structural description of MVs. We suggest to include confocal or electron microscopy characterizations to obtain an integrated analytical framework, as described in the data analysis protocol. Notably, the barrier thickness for quality MV barriers is readily determined by the onset in MV radius:

$$\delta_P \sim \frac{r_{0D}}{r_{0P}} \delta_D \quad \text{(Equation 8)}$$

with r_{0D} and r_{0P} the radii of the MV in the static assay and pressure assay, respectively. Note that this relationship is not valid for impermeable barrier made out of epithelial cells, for which $\delta_P/\delta_D > r_{0D}/r_{0P}$.

LIMITATIONS

This quantification protocol is only valid for good barriers (see troubleshooting 2).

This model assumes transcellular flux is negligible compared to paracellular flux, a reasonable approximation for HUVECs in monoculture conditions. However, this hypothesis may be erroneous, making the method to estimate pore size and density inconsistent.

The use of dextran tracers is a standard to study paracellular transport. The size (equivalently the molecular weight) of the polymer should be adapted according to the investigated tissue. For instance, low MW molecules would be required to assess the pore size of epithelial tissues, which are much more impermeable.

The model may not be valid for any type of supporting hydrogel. We describe the fabrication of MV in collagen gels, which are highly porous hydrogels. The high permeability of collagen gels of $\sim 10^{-13}$ m^2 is associated to a low hydraulic resistance in comparison to that of MVs, allowing us to detect leaky barriers with intraluminal pressure. Synthetic hydrogels (e.g., gelatin methacrylate or polyacrylamide), not to tell about hydrophobic gels such as silicone, that feature much lower permeability, are unlikely relevant to validate the quality of MVs.

MVs, as fabricated in this report, are cultured in static conditions without any shear flow. We have not attempted to evaluate the consequence of this physiological cue on the barrier function. Several reports have suggested to use a rocker to force a flow in the lumen. This simple approach can in principle be implemented with the technology described in this report, though we did not perform this development.

TROUBLESHOOTING

Problem 1

Bubbles can be detected in the collagen after the fabrication (related to Step 16).

Potential solution

- Place the chip in the fridge for 2 h to dissolve bubbles.
- If the cell loading is operated after 3–4 days, bubbles will disappear in the incubator.

Problem 2

Low density of HUVECs during MV fabrication (related to Step 31, middle panel of Figure 2).

Potential solution

- Repeat the loading of HUVECs one more time.
- Pass the cell suspension through the strainer before each loading step in order to avoid cell aggregation. Aggregates do not fill the voids on the luminal surface.

Problem 3

The MV is clogged by cells at the end of the loading process (related to Step 34, bottom panel of Figure 2).

Potential solution

- Insert a sterile needle in the vessel to disrupt the cell aggregate that blocks the lumen.

Problem 4

The MV is clogged by bubbles at the end of the loading process (related to Step 34).

Potential solution

- Add 10 μL of 3% dextran EGM-2 solution in the lateral reservoir the further away from the bubble.
- In most cases, the bubble will not be removed. It is then recommended to clean the silicone chip, remove the collagen gel, and use a plasma cleaning step.

Problem 5

Leaky MV when performing the macromolecular assays (related to Step 44).

Potential solution

- A leaky MV is characterized by large pores with a strong heterogeneity that is not compatible with the proposed model.
- The main explanation is the low density of cells during the seeding step. The fabrication should be started over again with attention to the homogeneity of cell attachment in the vessel.

RESOURCE AVAILABILITY

Lead contact

Further information and requests for resources and reagents should be directed to and will be fulfilled by the lead contact, Aurélien Bancaud (abancaud@laas.fr).

Technical contact

Further information and requests for material design and protocol implementation should be directed and will be fulfilled by the technical contact, Jean Cacheux (cacheux.jean@gmail.com).

Materials availability

All reagents generated in this study are available from the lead contact with a completed Materials Transfer Agreement. We are glad to share all reagents with compensation by requestor for shipping.

Data and code availability

- Microscopy data reported in this paper will be shared by the lead contact upon request.
- The code for image analysis is stored with the https://doi.org/10.17632/2rs7y84njn.1.
- Any additional information required to reanalyze the data reported in this work paper is available from the lead contact upon request.

SUPPLEMENTAL INFORMATION

Supplemental information can be found online at https://doi.org/10.1016/j.xpro.2024.102950.

ACKNOWLEDGMENTS

J.C. acknowledges the JSPS for postdoctoral fellowship. D.A. acknowledges the WINGS-QSTEP program for doctoral fellowship. This research was partly supported by the Grant-in-Aid for JSPS Fellows (20F20806), AMED P-CREATE (JP18cm0106239h0001), and JSPS Core-to-Core Program (JPJSCCA20190006). The authors thank the LIMMS (CNRS-Institute of Industrial Science, The University of Tokyo) for financial support and Eri Otsuka for technical assistance.

AUTHOR CONTRIBUTIONS

J.C., A.B., and Y.T.M. conceived and supervised the project; T.N., T.S., J.C., and A.B. developed the microvessel formation protocol; K.D. fabricated the injection reservoirs; J.C., A.B., and D.A. performed the experiments; J.C. and A.B. developed the mathematical model and analyzed the data; J.C. wrote the original draft; and J.C., A.B., D.A., T.N., T.S., K.D., and Y.T.M. contributed to writing – review and editing.

DECLARATION OF INTERESTS

The authors declare no competing interests.

REFERENCES

1. Cacheux, J., Bancaud, A., Alcaide, D., Suehiro, J.-I., Akimoto, Y., Sakurai, H., and Matsunaga, Y.T. (2023). Endothelial tissue remodeling induced by intraluminal pressure enhances paracellular solute transport. iScience *26*, 107141. https://doi.org/10.1016/j.isci.2023.107141.

2. Pauty, J., Usuba, R., Cheng, I.G., Hespel, L., Takahashi, H., Kato, K., Kobayashi, M., Nakajima, H., Lee, E., Yger, F., et al. (2018). A Vascular Endothelial Growth Factor-Dependent Sprouting Angiogenesis Assay Based on an In Vitro Human Blood Vessel Model for the Study of Anti-Angiogenic Drugs. EBioMedicine *27*, 225–236. https://doi.org/10.1016/j.ebiom.2017.12.014.

3. Pauty, J., Usuba, R., Takahashi, H., Suehiro, J., Fujisawa, K., Yano, K., Nishizawa, T., and Matsunaga, Y.T. (2017). A Vascular Permeability Assay Using an In Vitro Human Microvessel Model Mimicking the Inflammatory Condition. Nanotheranostics *1*, 103–113. https://doi.org/10.7150/ntno.18303.

4. Yoshimatsu, Y., Kimuro, S., Pauty, J., Takagaki, K., Nomiyama, S., Inagawa, A., Maeda, K., Podyma-Inoue, K.A., Kajiya, K., Matsunaga, Y.T., and Watabe, T. (2020). TGF-beta and TNF-alpha cooperatively induce mesenchymal transition of lymphatic endothelial cells via activation of Activin signals. PLoS One *15*, e0232356. https://doi.org/10.1371/journal.pone.0232356.

5. Nakajima, T., Sasaki, K., Yamamori, A., Sakurai, K., Miyata, K., Watanabe, T., and Matsunaga, Y.T. (2020). A simple three-dimensional gut model constructed in a restricted ductal microspace induces intestinal epithelial cell integrity and facilitates absorption assays. Biomater. Sci. *8*, 5615–5627. https://doi.org/10.1039/D0BM00763C.

6. Dechadilok, P., and Deen, W.M. (2006). Hindrance Factors for Diffusion and Convection in Pores. Ind. Eng. Chem. Res. *45*, 6953–6959. https://doi.org/10.1021/ie051387n.

7. Rippe, B., and Haraldsson, B. (1994). Transport of macromolecules across microvascular walls: the two-pore theory. Physiol. Rev. *74*, 163–219. https://doi.org/10.1152/physrev.1994.74.1.163.